

Training-and-prompt-free General Painterly Harmonization Using Image-wise Attention Sharing

Teng-Fang Hsiao
National Yang Ming Chiao Tung
University
bluedyee.ee09@nycu.edu.tw

Bo-Kai Ruan
National Yang Ming Chiao Tung
University
bkruan.ee11@nycu.edu.tw

Hong-Han Shuai
National Yang Ming Chiao Tung
University
hhshuai@nycu.edu.tw

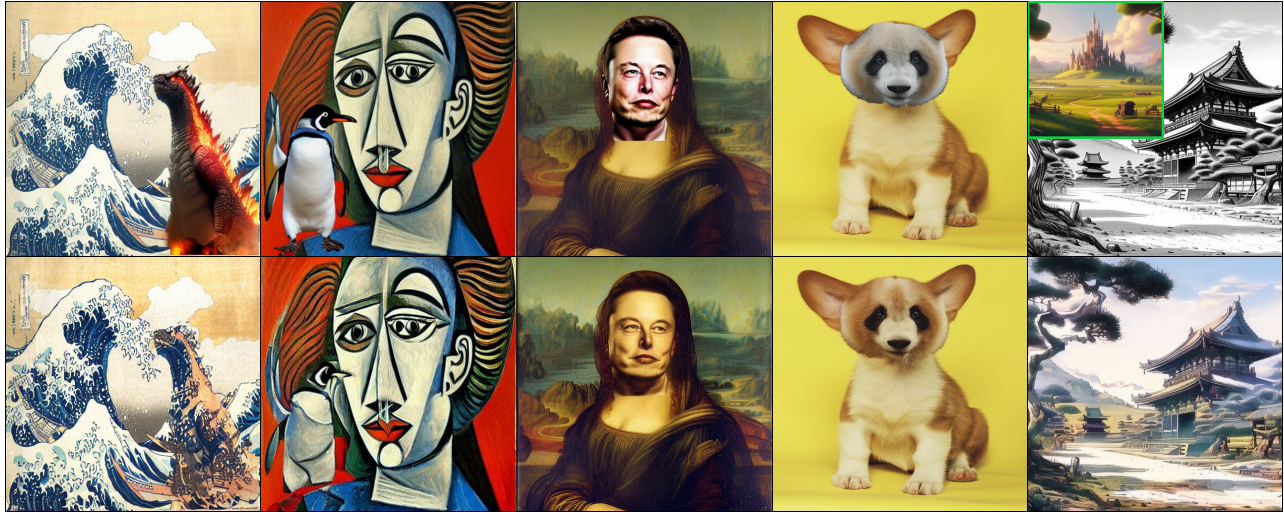


Figure 1: An illustrative example showcasing three fundamental tasks in general painterly harmonization: Object Insertion (columns 1 and 2), Object Swapping (columns 3 and 4), and Style Transfer (final column). The top row displays user-created composite images, with the last column’s green box highlighting the background reference. The bottom row reveals the results of our method, adeptly blending the morphology of the inserted object, the semantics of the background and the overall style.

ABSTRACT

Painterly Image Harmonization aims at seamlessly blending disparate visual elements within a single coherent image. However, previous approaches often encounter significant limitations due to training data constraints, the need for time-consuming fine-tuning, or reliance on additional prompts. To surmount these hurdles, we design a Training-and-prompt-Free General Painterly Harmonization method using image-wise attention sharing (TF-GPH), which integrates a novel “share-attention module”. This module redefines the traditional self-attention mechanism by allowing for comprehensive image-wise attention, facilitating the use of a state-of-the-art pretrained latent diffusion model without the typical training data limitations. Additionally, we further introduce “similarity reweighting” mechanism enhances performance by effectively harnessing cross-image information, surpassing the capabilities of fine-tuning or prompt-based approaches. At last, we recognize the deficiencies in existing benchmarks and propose the ‘General Painterly Harmonization Benchmark’, which employs range-based evaluation metrics to more accurately reflect real-world application. Extensive experiments demonstrate the superior efficacy of our method across various benchmarks. The code and web demo are available at <https://github.com/BlueDyee/TF-GPH>.

CCS CONCEPTS

• Computing methodologies → Computer vision; Image processing; • Applied computing → Fine arts.

KEYWORDS

diffusion model, attention, image editing, image harmonization, painterly harmonization, style transfer

1 INTRODUCTION

Image composition, the art of blending a foreground element from another image with a different background, frequently results in composite images marked by discordant color and illumination between the foreground and background. This discordance can render the composite image inharmonious and unrealistic. To mitigate these issues, image harmonization techniques have been developed, aiming to adjust the foreground appearance to seamlessly blend with its background [8, 30, 52, 54, 57, 58]. A specific subset of this field, painterly image harmonization, focuses on the integration of photographic elements into paintings, thereby facilitating artistic edits [5, 37, 39, 45, 62]. For example, [5] introduces a novel approach utilizing a dual-domain generator and discriminator to enhance visual harmony across both spatial and frequency domains. Furthermore, [37] unveils PHDiffusion, a model that incorporates a

lightweight adaptive encoder and a dual encoder fusion module, striking a better balance between style adaptation and content preservation in the realm of painterly image harmonization.

Despite notable advancements, current painterly image harmonization techniques struggle with generalizability, particularly when confronted with novel art styles or unique content compositions. A promising direction to overcome this limitation is the adoption of one-shot style transfer techniques, as suggested by VCT [9], which facilitate model adaptation through fine-tuning with a single style image. This approach enables networks to reimagine content images by applying stylistic elements learned from the style reference. However, this fine-tuning requirement significantly decreases its practicality and flexibility, as each style requires an additional training process that incurs computational costs 10 to 1000 times higher than a single inference process alone. Currently, the rise of multi-modality models has inspired alternative strategies, such as leveraging text-guided image synthesis to convey style nuances [18, 28, 38]. For example, TF-ICON [38] employs carefully crafted text prompts to guide the stylistic integration of objects into their new backgrounds. Yet, the effectiveness of this approach is hindered by the inherent challenge of encapsulating complex visual styles—spanning texture, color gradients, and spatial arrangements—through textual descriptions alone, highlighting the difficulty of translating the multifaceted nature of visual styles into precise and unambiguous textual prompts.

In this work, we propose **TF-GPH**, a novel diffusion pipeline that operates without the need for additional training or prompts, harnessing the capabilities of the pretrained latent diffusion model [47]. Notably, TF-GPH stands as a comprehensive solution, adept at executing a broad spectrum of painterly harmonization tasks, ranging from object insertion and swapping to full style transfers, as demonstrated in Fig. 1. This unified approach not only maintains the computational efficiency of its foundational diffusion pipeline, but also sets new benchmarks, surpassing previous methodologies in diverse evaluations. Specifically, at the core of our innovation is the enhancement of the conventional self-attention mechanism within the diffusion architecture. We introduce a novel **share attention layer**, engineered to facilitate image-wise rather than patch-limited attention modulation, enabling the composition image to directly attend to both content and style references, eliminating the need of the fine-tuning process to encode style information into diffusion model. Moreover, instead of leveraging the hard-attention adjustments found in prior work [7, 17, 18, 38, 55] to adjust the attention weight toward both content and style references, we further propose the **similarity reweighting** technique for balancing the attention weight toward both content and style references by scaling the similarity based on given hyperparameters. As such, a controllable harmonic integration of reference image styles can be achieved without the need of additional cross-attention output from prompt. This mechanism gives users the flexibility to subtly influence the intensity of the style, tailoring the output to various artistic preferences by adjusting the hyperparameters.

Finally, a critical challenge in the evaluation of painterly harmonization lies in the limited diversity of test data styles, which are often constrained to the styles seen during training (e.g., the pairing of WikiArt [53] with COCO [35]). This limitation poorly reflects the broad spectrum of styles encountered in real-world scenarios, such

as manga or sumi-e, which typically fall outside the distribution of common datasets. To bridge this gap and more accurately assess the zero-shot capabilities of **TF-GPH**, we introduce the “General Painterly Harmonization Benchmark” (GPH Benchmark). This new benchmark is designed not only to encompass a trio of harmonization tasks—object insertion, object swapping, and style transfer, but also to include different content and style references, thereby ensuring a robust and comprehensive evaluation framework. The validity and effectiveness of the GPH Benchmark are further substantiated through detailed qualitative and quantitative analysis presented in Sec. 5. Additionally, existing metrics solely emphasize either content or style similarity without adequately addressing user preference, i.e., different balances between stylization and content preservation for different samples. To link quantitative indices with user experience, we advocate for the adoption of range-based metrics. The range-based metrics compute both the lower bound and upper bound of the stylization and content-preservation strength among given data, viewing the applicable range as an indicator of adaptability across various scenarios; the wider range should be able to cater to more niches. Our contributions can be summarized as follows:

- (1) We introduce the **TF-GPH** framework, the first training- and-prompt-free pipeline using a diffusion model designed for general painterly harmonization.
- (2) Our proposed **share-attention layer with similarity reweighting** not only shows promising results in painterly harmonization tasks, but can serve as a more general form of the self-attention layer, providing a flexible option for attention-based image editing methods.¹
- (3) We propose the **GPH Benchmark**, consisting of various data for real-world usage, together with a range-based metric to align model performance with user experience.

2 RELATED WORK

2.1 Image Harmonization.

Image Harmonization can be divided into two main categories: **Realistic Image Harmonization** and **Painterly Image Harmonization**. Realistic Image Harmonization methods [2, 8, 10, 22, 26, 34, 44, 58, 61, 62], focus on blending objects into new backgrounds with an emphasis on consistent illumination, edge alignment, and shadow integrity. On the other hand, Painterly Image Harmonization [5, 37, 41, 45, 54, 57, 59], aims to artistically integrate objects into paintings, centering on stylistic congruence rather than realistic alignment, and strives to merge both artistic styles and textures, as seen in GP-GAN [57] which innovates by incorporating Poisson gradients into the training loss to enhance style blending. PHD-Net [5] advances this by integrating style loss [16] and the AdaIN module [24] for more refined style adaptation. Furthermore, PHD-diffusion [37] represents a significant pivot by adapting the GAN framework to a diffusion model with an adaptive encoder. Despite their advancements, these methods predominantly rely on extensive training processes, potentially limiting their adaptability to novel styles. In contrast, our proposed method eliminates the need

¹Due to the space constraint, please refer to the experiments in Appendix H of the supplementary materials.

for training, offering direct application to unseen styles, thereby broadening the scope and utility of painterly image harmonization.

2.2 Style Transfer.

Style transfer aims to modify the style of a content image to reflect a specified reference style, with existing methods generally falling into two categories: optimization-based and feedforward-based. Optimization-based techniques, such as [16, 28, 31], refine the image by aligning it with features extracted from the style reference; for instance, CLIPStyler [28] leverages a pre-trained CLIP model [46] for this purpose. Conversely, feedforward-based approaches, like StyTr² [12], utilize a Vision Transformer (ViT)-based architecture to reconstruct the content image using style feature patches. Among these, QuantArt [23] uniquely employ the vector quantization strategy to finely balance content preservation with style. Additionally, with the evolution of diffusion models, methods like VCT [9] and InST [64] have emerged, advocating for the fine-tuning of generative models with a style reference to embed style directly into the model’s architecture. Our proposed TF-GPH method, in contrast, delivers superior performance across a variety of benchmarks without the necessity for fine-tuning, significantly reducing the time required for style transformation.

2.3 Attention-based Image Editing

Manipulation of self-attention and cross-attention layers within diffusion UNet architectures is a common strategy in contemporary image editing methodologies [7, 14, 17, 18, 38, 55]. Notable examples include P2P [18], which employs prompt-driven cross-attention to modify objects within images, and PhotoSwap [17], which utilizes a fine-tuning approach [48] to position personal input references effectively. Similarly, TF-ICON [38] integrates both self-attention and cross-attention outputs into its diffusion model to seamlessly integrate objects into various backgrounds without the need for additional training, closely aligning our approach. However, all the methods like P2P, PhotoSwap, and TF-ICON depend on prompts that describe the image, which can pose challenges when suitable prompts are unavailable. In contrast, our TF-GPH method eliminates the need for such prompts, relying solely on image inputs and thus enhancing its applicability to a broader range of scenarios.

3 PRELIMINARY

3.1 Diffusion Probabilistic Models

Our approach leverages advances in the forefront of image generation technology, specifically through the implementation of diffusion probabilistic models (DPMs) [13, 20, 43, 47, 50]. The underlying concept behind DPMs is straightforward but powerful: it systematically reduces noise within an image in a stepwise manner. Within the framework of score-based methodologies [27, 36, 51], the diffusion process for a specific time step $t \in [0, T]$ can be encapsulated by the following stochastic differential equation (SDE):

$$dx_t = f(x_t, t)dt + g(t)dw_t, \quad (1)$$

where w_t denotes the standard Wiener process, $f(x_t, t)$ is identified as the drift coefficient describing the distribution shift and $g(t)$ represents the diffusion coefficient that modulates the intensity of

the noise. To counteract the initial noise and restore the image to its original state, a reverse-time SDE is employed:

$$dx_t = [f(x_t, t) - g(t)^2 \nabla \log p_t(x_t)] dt + g(t) d\bar{w}_t, \quad (2)$$

where $\nabla \log p_t(x_t)$ is the scoring function, often approximated by a neural network, denoted as $\epsilon_\theta(x_t, t)$. The model parameters, represented by θ , are optimized through a noise reduction training objective [20, 51], which facilitates the conversion of noisy inputs back to their original noise-free counterparts. Throughout this paper, we follow the Variance Preserving SDE [51] form.

3.2 DPM Inversion

In the domain of diffusion-based image editing [6, 11, 17, 18, 29, 32, 38, 49], inversion plays a crucial role. Successful inversion signifies the model’s capability to regenerate a reference image, thereby enabling modifications in the regenerated image to effectuate property alterations in the edited output. Conventional approaches predominantly utilize the DDIM [50] to reversibly return the image to its noise form through an ordinary differential equation:

$$dx_t = [f(x_t, t) - g(t)^2 \nabla \log p_t(x_t)] dt. \quad (3)$$

However, the efficacy of DDIM diminishes when the images is out of distribution, necessitating additional fine-tuning [17, 48, 49]. Addressing this limitation, DPM-Solver++ [36] emerges as a solution, which we adopt for reconstruction, adept at inverting images across a wider array of distributions without the prerequisite of fine-tuning [17, 48, 49], even in scenarios involving personalized input. In order to improve the stability of the inversion process, TF-ICON [38] introduces the use of an exceptional prompt embedding $\rho_{\text{exceptional}}$, which differs from the conventional null prompt ϕ , aligning more congruently with the mechanics of native generation.

4 METHOD

Our research aims to facilitate a general form of painterly harmonization based on images only without the additional need for prompts, which can facilitate a variety of applications, *i.e.*, the insertion of objects, object swapping, and style transfer. Formally, given a background painting I^b , a foreground object image I^f , and I^{comp} , which is the user-specified composition that guides the size and position of the foreground object on the background painting, the goal of painterly harmonization is to transfer the style from I^b to the object in I^{comp} seamlessly, resulting a harmonized image I^o .

To address the challenge of painterly harmonization, we introduce a novel framework titled Training-and-Prompt-Free General Painterly Harmonization using a Diffusion Model (TF-GPH), as depicted in Fig. 2. Our method ingeniously leverages a diffusion model to harmonize elements within a painterly composition without the need for explicit training or user-defined prompts. Specifically, the inputs—foreground I^f , background I^b , and composite I^{comp} —are initially processed through an inversion mechanism equipped with either a standard null prompt embedding or a predefined exceptional prompt embedding $\rho_{\text{exceptional}}$, which has demonstrated its ability for stabilizing inversion process [38]. Subsequently, a denoising operation is applied concurrently to all three images, during which the composite image I^{comp} is enriched with style attributes.

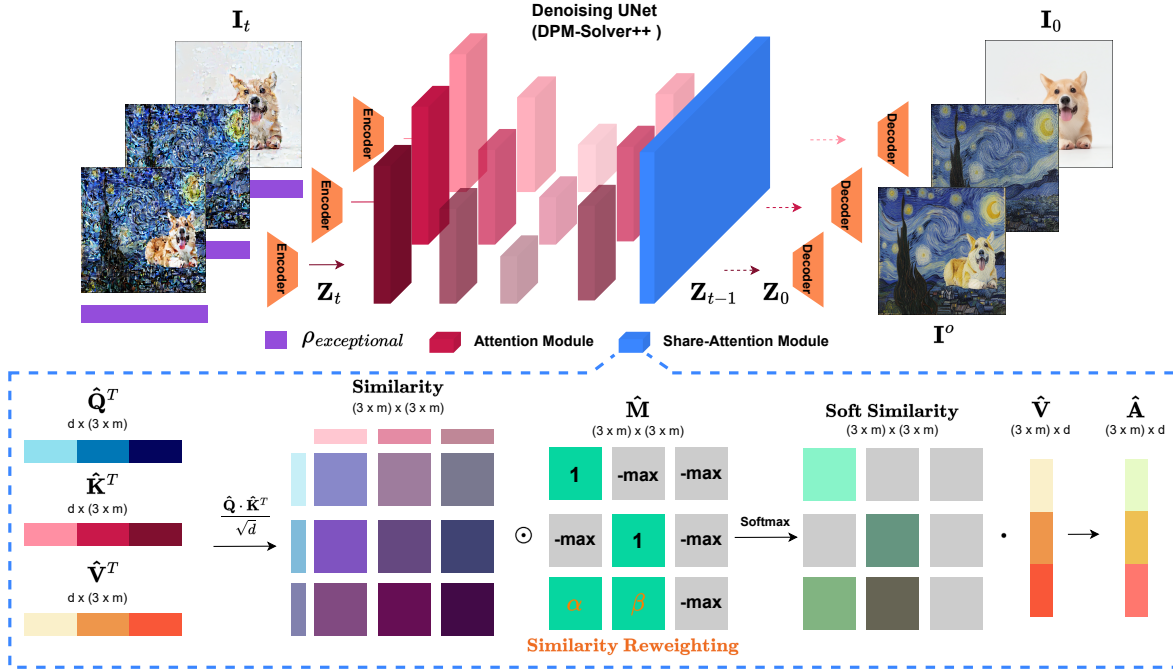


Figure 2: The architecture of our proposed TF-GPH method involves several stages. Initially, we feed the denoising U-Net with the inverse latent Z_t , and during the first $l < L_{\text{share}} - 1$ layers of the U-Net, the three latent representations, z_t^f , z_t^b , and z_t^{comp} , are forwarded separately to the Attention Module. Afterward, they are fed into the Share-Attention Module (the blue part below), obtaining their image-wise attention via Eq. (5). In the end, the output harmonized image I^o is produced.

The core of our architecture is the **Shared Attention Module**, a novel component designed to extract and amalgamate the foreground object details from I^f with the stylistic elements of I^b , ensuring the coherence of the final output I^o . This integration is further refined through our **Similarity Reweighting** technique, which optimizes the attention matrix to resonate with the underlying feature distribution more effectively. Although our framework is versatile enough to support both object swapping and style transfer—with the former viewed as a semantically richer variant of object insertion and the latter as a broader aspect of the same—our discussion here is confined to object insertion for brevity.

4.1 Share-Attention Module

In the framework of diffusion models, the attention mechanisms [56] are essential to capture characteristic details, facilitating both the elimination of noise and the enhancement of context information. Specifically, the self-attention module plays a vital role in synthesizing the output by internalizing and using the inherent data characteristics, while the cross-attention module is instrumental in incorporating contextual information from various modalities, e.g., images, text, and audio, thus amplifying the conditional impact on the resultant images. Since our approach does not need an additional prompt to guide the fusion, we can simply utilize self-attention to ensure that the background style is harmonically fused into the composition image during the denoising process.

Given three input images I^f , I^b , and I^{comp} , these images are first compressed by a VAE encoder [47] into latent representations

$z_0^f \in \mathbb{R}^{w \times h \times d}$, $z_0^b \in \mathbb{R}^{w \times h \times d}$, $z_0^{\text{comp}} \in \mathbb{R}^{w \times h \times d}$, respectively, where w and h denote the width and height of the latent shape, d is the feature channels and the subscript 0 denotes the initial timestep of the diffusion process. Next, we apply the DPM-Solver++ inversion to convert the initial latents z_0^f , z_0^b , and z_0^{comp} to noisy latents z_T^f , z_T^b , and z_T^{comp} , where $z_T \sim N(0; \sigma_T^2)$. This preprocess enabling the image modification during subsequent reconstruction process.

During the reconstruction process from the time step T to 0, we incorporate the style feature into z_t^{comp} using our proposed shared attention module. This module can be viewed as a more general form of the self-attention module, allowing for feature flow between images within the same batch. Specifically, the traditional self-attention module projects the input feature $z \in \mathbb{R}^{m \times d}$ of length $m = (w \cdot h)$ onto the corresponding $Q, K, V \in \mathbb{R}^{m \times d}$ through learned linear layers inside the original self-attention module and computes the attention matrix $A \in \mathbb{R}^{m \times d}$ as follows.

$$A(Q, K, V) = \text{Softmax} \left(QK^T / \sqrt{d} \right) V, \quad (4)$$

To enable the flow of feature information between images during the attention operation, we should consider three images at the same time instead of processing each attention matrix independently. To create the query, key, and value from three different inputs, we first concatenate three input latents on the first dimension to form $Z_T \in \mathbb{R}^{(3 \cdot m) \times d} = [z_T^f, z_T^b, z_T^{\text{comp}}]$. Then we project the latent Z_T into the corresponding $\hat{Q}, \hat{K}, \hat{V} \in \mathbb{R}^{(3 \cdot m) \times d}$. However, directly feeding $\hat{Q}, \hat{K}, \hat{V}$ into Eq. (4) may disrupt the content of z^b

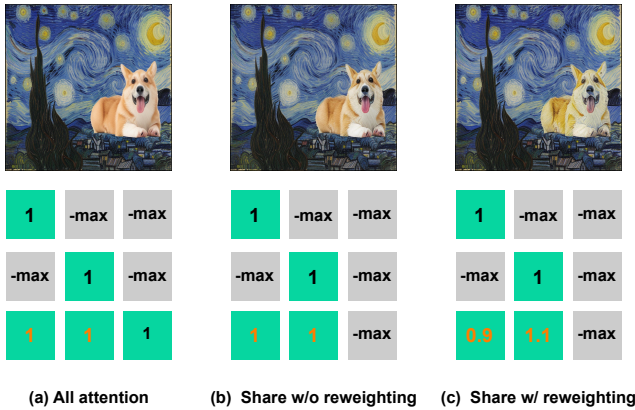


Figure 3: Comparisons of different attention strategy with corresponding similarity mask (read with Fig. 2).

and z^b since the additional attention from other images making the latent differ from original reconstruction without attention from others. To keep the content of z^f and z^b intact for correctly guiding the harmonization of z^{comp} , we propose a specially designed mask $\hat{M} \in \mathbb{R}^{(3 \cdot m) \times (3 \cdot m)}$ that allows z^{comp} to utilize information from z^f and z^b while keeping z^f and z^b intact. The shared attention equation is thus calculated by:

$$\hat{A}(\hat{Q}, \hat{K}, \hat{V}) = \text{Softmax} \left(\hat{M} \odot (\hat{Q}\hat{K}^T) / \sqrt{d} \right) \hat{V}, \quad (5)$$

where \odot denotes the Hadamard product. Afterward, Eq.(5) outputs the batch attention $\hat{A} \in \mathbb{R}^{(3 \cdot m) \times d}$ containing the intact A^f , A^b , and A^{comp} guided by the features of z^b and z^b . The specially designed \hat{M} can be visualized as:

$$\hat{M} = \begin{bmatrix} 1 \cdot J & v \cdot J & v \cdot J \\ v \cdot J & 1 \cdot J & v \cdot J \\ \alpha \cdot J & \beta \cdot J & \gamma \cdot J \end{bmatrix}$$

Here, $J \in \mathbb{R}^{m \times m}$ is an all-one matrix, and $v = -\infty$ minimizes the similarity between Q and K on the corresponding entry, keeping A^f , A^b intact. It is worth noting that when setting $\alpha = -\infty$, $\beta = -\infty$, and $\gamma = 1$, each row in Eq.(5) is equivalent to Eq. (4) as Q^{comp} , Q^f , and Q^b can only attend to its counterpart K^{comp} , K^f , and K^b without information from other images. Therefore, our proposed shared attention module can be viewed as an expansion of the self-attention layer with adjustable entries controlling image-wise attention sharing, which is also capable to be incorporated into other image editing methods (see Appendix H for more details).

4.2 Similarity Reweighting

A default approach to allow z^{comp} to attend to all three images simultaneously is to set α , β , and γ in M to 1 with the expectation that z^{comp} would be able to incorporate information from z^b and z^b , achieving stylized and harmonized output. However, as illustrated in Fig. 3(a), the output image I^o appears identical to the input composite image I^{comp} because the $Q^{\text{comp}}-K^{\text{comp}}$ pairs exhibit overwhelming similarity as compared to other pairs, thus dominating the entire reconstruction process. To fuse the images

more naturally, it is necessary to disentangle the overwhelming similarity caused by the $Q^{\text{comp}}-K^{\text{comp}}$ pairs while maintaining its original semantic information.

To eliminate the overwhelming issue, we propose to remove the similarity calculation of $(Q^{\text{comp}}, K^{\text{comp}})$ by setting $\gamma = -\infty$. Forcing Q^{comp} only be able to utilize the key and value "shared" by others (z^b and z^b), the result can be found in Fig. 3(b). The intriguing fact is that the output image only changes slightly even when the pasted "corgi" in I^{comp} has an absolutely different scale of background compared to the "corgi" in I^f . We infer that the failure of Fig. 3(b) is that the pretrained diffusion model is robust enough to capture high-level semantic and structural information even with minor disturbances, such as differences in scale and position. As such, the self-attention layer can withstand perturbations, generating results that are similar to the original input.

To decipher which perturbation level can break the self-attention robustness but still generate high-quality results. A simple idea with attention injection has been widely adopted by previous research [17, 18, 38, 55], which can be viewed as a strong perturbation of self-attention through additional information from other images. However, directly injecting additional attention does not blend well with the background image. The reason behind the malfunction of attention injection toward the self-attention layer is that the foreground and the background images lie in different distributions, causing its attention similarity low on others and overwhelmed by themselves. Hence, our share attention module cannot force the foreground to adapt the background style, as shown in Fig. 3(b).

To mitigate the gap between two distinct image distributions, we assign different values to α and β , ensuring that the merging of features occurs with variant weights, which forces the model to guide the image reconstruction in a predetermined direction. Specifically, α should be set to be greater than β , urging our model places greater emphasis on stylistic background features of z^b while maintaining the integrity of the foreground content. This methodology can be interpreted as an adaptation of the attention mechanism, achieved by altering the similarity relationship between features, a technique we call "soft injection." Unlike direct feature integration methods that rely on a copy-and-paste paradigm, soft injection provides weighted blending. Our observations reveal that soft injection facilitates superior image-wise self-attention editing, especially when compared with conventional prompt-wise cross-attention editing techniques [17, 18, 38, 55], thus giving more granular control over the editing process. We provide an illustration in Fig. 3(c) by setting $\alpha = 0.9$ and $\beta = 1.1$, we can strike a satisfactory balance, harmoniously blending the foreground and background features. The overall algorithm can be found in Appendix A.

5 EXPERIMENTS

5.1 Setup

We employ the Stable Diffusion model [47] as the pretrained backbone and utilize DPM Solver++ as the scheduler with a total of 25 steps for both inversion and reconstruction. Specifically, we first resize the input images I^f , I^b , and I^{comp} to 512×512 , and encode them into corresponding z_0^f , z_0^b , and z_0^{comp} . Afterward, we take these latents with prompt embedding $\rho_{\text{exceptional}}$ as the input of Stable Diffusion model during both inversion and reconstruction

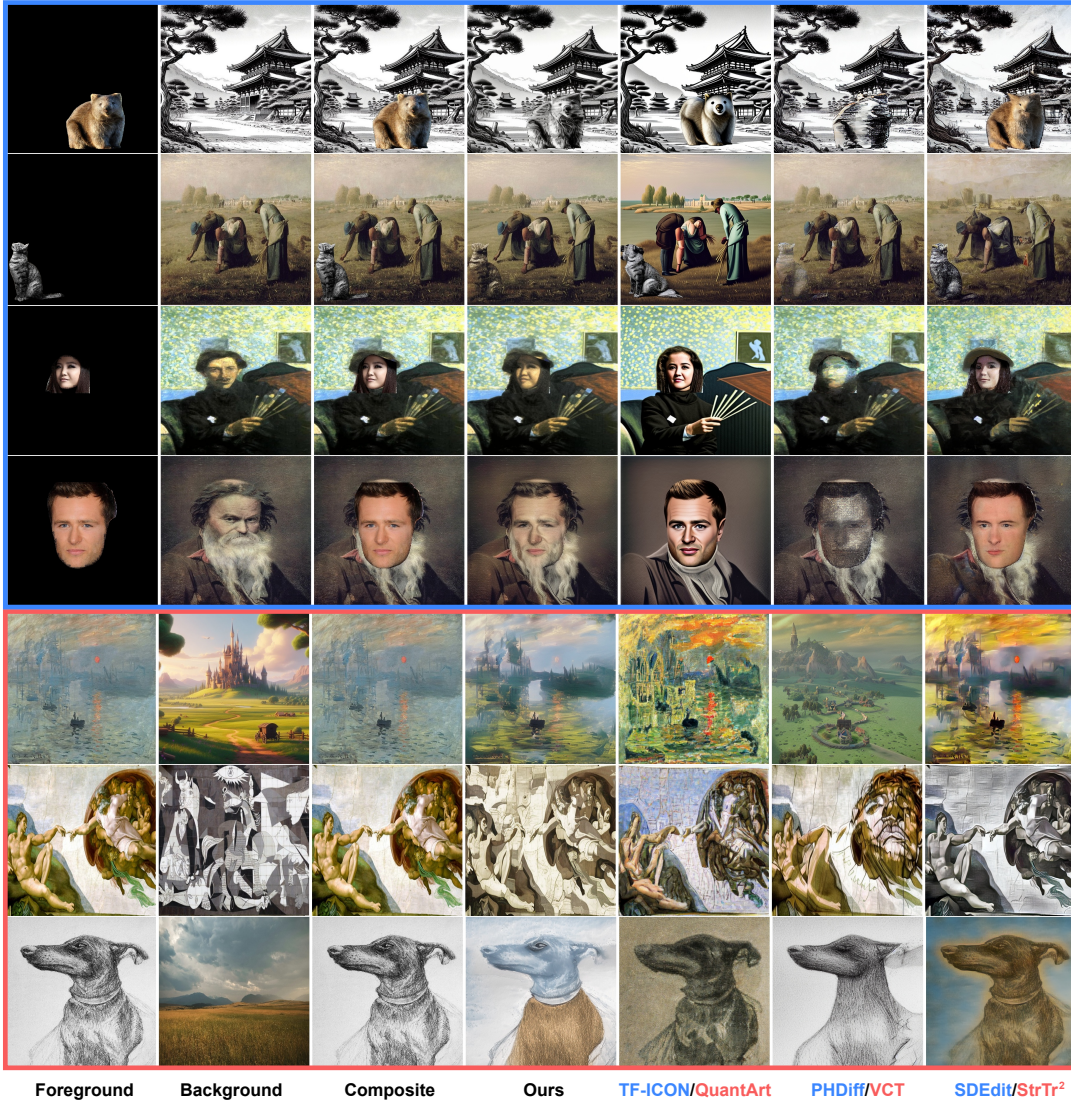


Figure 4: Qualitative result of **object insertion** (rows 1 and 2), **object swapping** (rows 3 and 4), and **style transfer** (rows 5-7)

Table 1: Quantitative results of GPH-Benchmark (\dagger represents the method with inference-time-adjustable hyperparameters. The left side of / represents content emphasis strategy, while the right side of / represents stylized emphasis strategy.

	Painterly Harmonization					Style Transfer			
	Ours \dagger	TF-ICON \dagger [38]	PHDiff \dagger [37]	PHDNet[5]	SDEdit[41]	Ours \dagger	QuantArt[23]	VCT \dagger [9]	StyTr 2 [12]
<i>Venue</i>	-	ICCV'23	MM'23	AAAI'23	ICLR'22	-	CVPR'23	ICCV'23	CVPR'22
$LP_{bg} \downarrow$	0.11/0.12	0.20/0.36	0.12/0.12	0.37	0.24	0.72/ 0.56	0.69	0.71/0.71	0.61
$LP_{fg} \downarrow$	0.10/0.32	0.32/0.36	0.10/0.39	0.41	0.21	0.11/0.45	0.51	0.11/0.32	0.40
$CP_{img} \uparrow$	95.42/78.63	85.35/82.05	95.13/73.65	78.85	87.55	96.43/69.57	80.27	95.54/73.91	83.57
$CP_{style} \uparrow$	47.50/ 56.37	47.66/47.40	47.64/55.96	50.62	49.28	57.97/ 78.60	64.59	59.25/67.04	63.28
$CP_{dir} \uparrow$	0.11/11.69	2.96/4.63	0.35/ 15.39	8.50	3.27	3.97/ 51.59	26.90	6.22/35.63	22.08

stage. For the style transfer task, we set α to 0.9, β to 1.1, T_{share} to 25 (we activate the share-attention layer when $t < T_{share}$), and L_{share} to 14 (out of 16 total layers in the diffusion U-Net). As for

the object swapping purpose, we change T_{share} to 20, and for the object insertion usage, we change T_{share} to 15. We refer to these hyperparameters (T_{share} , L_{share} , α , β) as “inference-time-adjustable

hyperparameters” since they can be flexibly adjusted to modulate the strength of style according to different use cases during the inference process. Due to the space constraint, please refer to Appendix G.1 in the supplementary materials for the sensitivity test on the hyperparameters.

5.2 Datasets and Metrics

Datasets. We generalize the computational metrics and benchmarks from various image editing methods: “Painterly image harmonization” [5, 37, 62], “Prompt-based image composition” [17, 38, 41], “Style Transfer” [9, 12, 23, 64], and our proposed “General Painterly Harmonization” achieved by the General Painterly Harmonization Benchmark (GPH Benchmark). This benchmark generalizes real-world usage scenarios of the aforementioned methods including “Object Insertion”, “Object Swapping” and “Style Transfer” providing a more practical benchmark for evaluating the applicability of cross-image editing methods and aims to mitigate the shortcomings of existing benchmarks such as WikiArt combined with COCO [35, 53] and the TF-ICON Benchmark [38]. Details of these datasets and the motivation of GPH Benchmark can be found in Appendix B.

LPIPS and CLIP regarding computation metrics. LPIPS [63] and CLIP [46] (abbreviated as LP and CP respectively in the subsequent discussion) are two widely utilized metrics for evaluating image similarity, each leveraging unique aspects of image analysis. LPIPS employs a pretrained model from ImageNet to extract deep features, assessing perceptual similarity based on these features. In contrast, CLIP, which is trained on a large-scale dataset of images and text, excels at capturing high-level semantic information in both visual and contextual domain. In TF-ICON benchmark [38], these two metrics are leveraged to assess content preservation and stylized performance, where LP_{fg} and CP_{img} are calculated to measure the content consistency and image semantic similarity, respectively. Moreover, LP_{bg} is also used to measure background consistency before and after harmonization. On the other hand, StyleGAN-NADA [15] proposes CP_{dir} to calculate the alignment level between the feature shift direction of pasted object and the background. Specifically, let $f(\cdot)$ denote the extracted feature of CLIP image encoder. The alignment level is calculated by the similarity between $\{f(I^o) - f(I^f)\}$ and $\{f(I^b) - f(I^f)\}$. Finally, following VCT [9], we adopt CP_{style} to measure the feature similarity of harmonized images and style references.

Range-based evaluation. While metrics such as LPIPS and CLIP are useful for assessing content fidelity and stylization in image harmonization, they can sometimes emphasize either too much content preservation or excessive stylization, as shown in Fig. 11. This imbalance may compromise the overall harmonization and visual quality of the output image. To address this issue, we propose that an effective general painterly harmonization pipeline should offer users the flexibility of balancing between stylization intensity and content integrity by adjusting hyperparameters. To quantitatively measure this capability, we suggest defining upper and lower bounds for content preservation and stylization, which can serve as indicators of a method’s adaptability across different harmonization scenarios. In other words, methods with a wider range should be able to adapt to more use cases. Besides, we have re-implemented

existing baselines with configurable hyperparameters to facilitate a range-based comparison.²

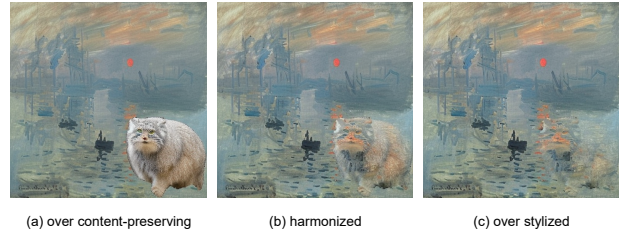


Figure 5: Comparison of different stylized strength.

5.3 Qualitative Comparison

For qualitative comparison, TF-GPH showcases remarkable capabilities in our proposed GPH Benchmark as depicted in Fig. 4, ranging from low-level texture harmonization like transitioning to singular colors and color matching (rows 1 and 2) to high-level semantic harmonization such as extending the skin color of the replaced man onto the pasted face or redrawing the covered beard along with the chin line of the pasted face (rows 3 and 4). While PHDiff and SDEdit are able to achieve low-level texture harmonization, they often struggle with high-level semantic blending, failing to successfully recover face feature. Additionally, our method is also able to seamlessly composites images without the need for prompts in TF-ICON Benchmark (see Appendix D.2) and showing outstanding performance in other existing dataset (see Appendix D.1). This highlights how our similarity reweighting technique effectively leverages the innate characteristics of the diffusion model to achieve both texture and semantic harmonization with image-wise attention.

Moreover, our proposed TF-GPH demonstrates exceptional performance in style transfer (row 5,6,7 in Fig. 4), utilizing a diverse range of graphic art forms within the test dataset. Our method excels at stylizing original content while maintaining superior image quality, by leveraging advanced diffusion image generation techniques. This addresses a notable limitation observed in non-diffusion methods such as QuantArt and StyTr², which often struggle to maintain image quality. Additionally, TF-GPH better preserves the layout of the content image compared to tuning-based diffusion editing methods like VCT, credits to its innovative share-attention layer. This layer effectively retains feature information from reference images during inference, thereby enhancing content detail in the generated output. More qualitative results are available in Appendix D.

5.4 Quantitative results

Tab. 1 and Tab. 2 showcase the quantitative results from our proposed GPH and TF-ICON Benchmark respectively. Notably, a detailed range-based evaluation on WikiArt combined with COCO is documented in Appendix E.1. TF-GPH consistently demonstrates superior performance across these benchmarks, outperforming existing evaluation criteria. Our uniquely designed share-attention

²More implementation details can be found in Appendix C.

module significantly enhances reference information retention compared to prompt-based editing methods like TF-ICON and SDEdit, improving LP_{bg} , LP_{fg} lower bounds by 45% and 52% at least. These methods often struggle to preserve details of the composite image when the prompts inadequately complement the reference images.

Furthermore, TF-GPH utilizes a pre-trained diffusion model augmented with a similarity reweighting mechanism, achieving higher stylization upper bounds than methods that require extensive training, such as QuantArt and StyTr². These conventional methods frequently encounter limitations in handling diverse styles within the test data, while our TF-GPH achieves a substantial improvement around 17% ~ 28% in CP_{style} and 44% ~ 133% in CP_{dir} upper bounds compared to other style transfer methods. Importantly, TF-GPH’s inference-time-adjustable hyperparameters enable it to offer the broadest range of content preservation and stylization capabilities, as evidenced in both Tab. 1 and Appendix E.1.

We also conduct a comprehensive user study to evaluate the efficacy of TF-GPH. The study encompasses two distinct evaluation tasks: Style Transfer and Painterly Harmonization, which includes object insertion and swapping. For this, we recruited 50 participants through Amazon MTurk, each tasked with responding to 10 questions. Participants were instructed to assess the generated images based on three criteria: (1) Content Consistency, (2) Style Similarity, and (3) Visual Quality, rating them on a scale from 1 (worst) to 4 (best). Specifically, for the Painterly Harmonization task, ‘Content Consistency’ was subdivided into ‘Object Consistency’ and ‘Background Consistency’.

Fig. 6(a) displays the results for the painterly harmonization task, where TF-GPH not only excels in stylization but also in preserving superior visual quality of the pasted objects. Additionally, Fig. 6(b) illustrates the outcomes for the style transfer task, with TF-GPH achieving the highest scores in overall quality and content consistency, along with competitive style similarity. These results validate our hypothesis that visual quality transcends mere content preservation or style strength. The consistently high performance across these metrics underlines the robustness of our method for diverse real-world applications. Further details on the methodology and results of the user study are provided in Appendix F.

5.5 Ablation Study

Tab. 3 reveals the impact of components within TF-GPH. Simply applying reconstruction to the composite image is ineffective at harmonizing pasted object into background. Additionally, incorporating a vanilla share-attention layer offers minimal improvement due to the inherent nature of the attention mechanism, as previously discussed. However, the integration of the similarity reweighting strategy within the share-attention layer allows the TF-GPH pipeline to successfully encode cross-image information into the composite image, resulting in significant enhancements in the stylization indexes CP_{style} and CP_{dir} across both tasks.

6 CONCLUSION

In this work, we introduce a novel **share-attention layer**, enabling the utilization of image-wise attention from different images. Furthermore, we devised the **similarity reweighting** technique capable of flexibly controlling the attention strength of reference

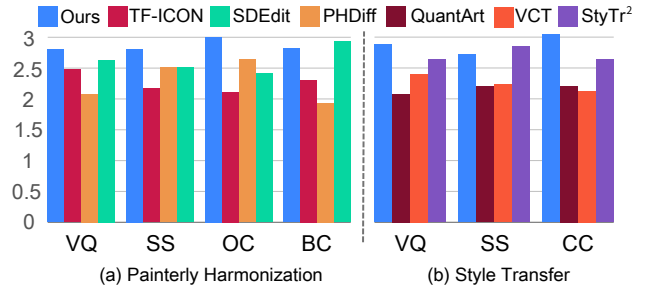


Figure 6: User study result, we abbreviate “Visual Quality”, “Style Similarity”, “Object Consistency”, “Background Consistency” and “Content Consistency” into “VQ”, “SS”, “OC”, “BC”, and “CC”, respectively.

Table 2: Quantitative result of TF-ICON Benchmark

Method	LP_{bg} ↓	LP_{fg} ↓	CP_{img} ↑	CP_{text} ↑
SDEdit (0.4)[41]	0.35	0.62	80.56	27.73
Blended[1]	0.11	0.77	73.25	25.19
Paint[60]	0.13	0.73	80.26	25.92
DIB[62]	0.11	0.63	77.57	26.84
TF-ICON[38]	0.10	0.60	82.86	28.11
Ours	0.05	0.48	83.34	30.33

Table 3: Ablation study on TF-GPH’s components in painterly harmonization (upper) and style transfer (bottom) on GPH. (We abbreviate “Share-Attention layer” and “Similarity Reweighting” as “SA” and “SR”)

Metrics	LP_{bg} ↓	LP_{fg} ↓	CP_{style} ↑	CP_{dir} ↑
Vanilla	0.11	0.09	47.50	0.11
+SA	0.11/0.11	0.10/0.10	47.50/47.50	0.11/0.18
+SR	0.11/0.12	0.10/0.32	47.50/56.37	0.11/11.69
Vanilla	0.72	0.11	57.97	3.97
+SA	0.72/0.69	0.11/0.12	57.97/59.05	3.97/5.12
+SR	0.72/ 0.56	0.11/0.45	57.97/ 78.60	3.97/ 51.59

images without the need for fine-tuning or prompt. Based on these innovations, we propose **TF-GPH** able to perform a more general form of the painterly harmonization task including object insertion, object swapping and style transfer. Furthermore, we construct the **GPH Benchmark** along with **range-based evaluation** aiming to mitigate the current shortage of evaluations for image editing methods. We believe that TF-GPH provides ordinary users with more convenience for content creation, and our contributions can facilitate growth in future research on image editing methods. In the future, we plan to further explore the potential extensions of share-attention layer to other attention-based applications and modalities, such as 3D generation [4, 33, 42] and video creation [3, 19, 21].

REFERENCES

- [1] Omri Avrahami, Ohad Fried, and Dani Lischinski. 2023. Blended latent diffusion. *ACM Transactions on Graphics (TOG)* 42, 4 (2023), 1–11.
- [2] Samaneh Azadi, Deepak Pathak, Sayna Ebrahimi, and Trevor Darrell. 2020. Compositional gan: Learning image-conditional binary composition. *International Journal of Computer Vision* 128 (2020), 2570–2585.
- [3] Andreas Blattmann, Robin Rombach, Huan Ling, Tim Dockhorn, Seung Wook Kim, Sanja Fidler, and Karsten Kreis. 2023. Align your latents: High-resolution video synthesis with latent diffusion models. In *Proceedings of the IEEE/CVF Conference on Computer Vision and Pattern Recognition*. 22563–22575.
- [4] Shengqu Cai, Eric Ryan Chan, Songyou Peng, Mohamad Shahbazi, Anton Obukhov, Luc Van Gool, and Gordon Wetzstein. 2023. Diffdreamer: Towards consistent unsupervised single-view scene extrapolation with conditional diffusion models. In *Proceedings of the IEEE/CVF International Conference on Computer Vision*. 2139–2150.
- [5] Junyan Cao, Yan Hong, and Li Niu. 2023. Painterly image harmonization in dual domains. In *Proceedings of the AAAI Conference on Artificial Intelligence*, Vol. 37. 268–276.
- [6] Mingdeng Cao, Xintao Wang, Zhongang Qi, Ying Shan, Xiaohu Qie, and Yinqiang Zheng. 2023. Masactrl: Tuning-free mutual self-attention control for consistent image synthesis and editing. In *Proceedings of the IEEE/CVF International Conference on Computer Vision*. 22560–22570.
- [7] Hila Chefer, Yuval Alaluf, Yael Vinker, Lior Wolf, and Daniel Cohen-Or. 2023. Attend-and-excite: Attention-based semantic guidance for text-to-image diffusion models. *ACM Transactions on Graphics (TOG)* 42, 4 (2023), 1–10.
- [8] Haoxing Chen, Zhangxuan Gu, Yaohui Li, Jun Lan, Changhua Meng, Weiqiang Wang, and Huaxiong Li. 2023. Hierarchical dynamic image harmonization. In *Proceedings of the 31st ACM International Conference on Multimedia*. 1422–1430.
- [9] Bin Cheng, Zuhao Liu, Yunbo Peng, and Yue Lin. 2023. General image-to-image translation with one-shot image guidance. In *Proceedings of the IEEE/CVF International Conference on Computer Vision*. 22736–22746.
- [10] Wenyan Cong, Jianfu Zhang, Li Niu, Liu Liu, Zhixin Ling, Weiyan Li, and Liqing Zhang. 2020. Dovenet: Deep image harmonization via domain verification. In *Proceedings of the IEEE/CVF conference on computer vision and pattern recognition*. 8394–8403.
- [11] Guillaume Couairon, Jakob Verbeek, Holger Schwenk, and Matthieu Cord. 2023. DiffEdit: Diffusion-based Semantic Image Editing with Mask Guidance. In *International Conference on Learning Representations*.
- [12] Yingying Deng, Fan Tang, Weiming Dong, Chongyang Ma, Xingjia Pan, Lei Wang, and Changsheng Xu. 2022. Stytr2: Image style transfer with transformers. In *Proceedings of the IEEE/CVF conference on computer vision and pattern recognition*. 11326–11336.
- [13] Prafulla Dhariwal and Alexander Nichol. 2021. Diffusion models beat gans on image synthesis. *Advances in neural information processing systems* 34 (2021), 8780–8794.
- [14] Dave Epstein, Allan Jabri, Ben Poole, Alexei Efros, and Aleksander Holynski. 2023. Diffusion self-guidance for controllable image generation. *Advances in Neural Information Processing Systems* 36 (2023), 16222–16239.
- [15] Rinon Gal, Or Patashnik, Haggai Maron, Amit H Bermano, Gal Chechik, and Daniel Cohen-Or. 2022. Stylegan-nada: Clip-guided domain adaptation of image generators. *ACM Transactions on Graphics (TOG)* 41, 4 (2022), 1–13.
- [16] Leon A Gatys, Alexander S Ecker, Matthias Bethge, Aaron Hertzmann, and Eli Shechtman. 2017. Controlling perceptual factors in neural style transfer. In *Proceedings of the IEEE conference on computer vision and pattern recognition*. 3985–3993.
- [17] Jing Gu, Yilin Wang, Nanxuan Zhao, Tsu-Jui Fu, Wei Xiong, Qing Liu, Zhifei Zhang, He Zhang, Jianming Zhang, HyunJoon Jung, et al. 2024. Photoswap: Personalized subject swapping in images. *Advances in Neural Information Processing Systems* 36 (2024).
- [18] Amir Hertz, Ron Mokady, Jay Tenenbaum, Kfir Aberman, Yael Pritch, and Daniel Cohen-or. 2023. Prompt-to-Prompt Image Editing with Cross-Attention Control. In *International Conference on Learning Representations*.
- [19] Jonathan Ho, William Chan, Chitwan Saharia, Jay Whang, Ruiqi Gao, Alexey Gritsenko, Diederik P Kingma, Ben Poole, Mohammad Norouzi, David J Fleet, et al. 2022. Imagen video: High definition video generation with diffusion models. *arXiv preprint arXiv:2210.02303* (2022).
- [20] Jonathan Ho, Ajay Jain, and Pieter Abbeel. 2020. Denoising diffusion probabilistic models. *Advances in neural information processing systems* 33 (2020), 6840–6851.
- [21] Jonathan Ho, Tim Salimans, Alexey Gritsenko, William Chan, Mohammad Norouzi, and David J Fleet. 2022. Video diffusion models. *Advances in Neural Information Processing Systems* 35 (2022), 8633–8646.
- [22] Yan Hong, Li Niu, and Jianfu Zhang. 2022. Shadow generation for composite image in real-world scenes. In *Proceedings of the AAAI conference on artificial intelligence*, Vol. 36. 914–922.
- [23] Siyu Huang, Jie An, Donglai Wei, Jiebo Luo, and Hanspeter Pfister. 2023. QuantArt: Quantizing image style transfer towards high visual fidelity. In *Proceedings of the IEEE/CVF Conference on Computer Vision and Pattern Recognition*. 5947–5956.
- [24] Xun Huang and Serge Belongie. 2017. Arbitrary style transfer in real-time with adaptive instance normalization. In *Proceedings of the IEEE international conference on computer vision*. 1501–1510.
- [25] Jaeseok Jeong, Mingi Kwon, and Youngjung Uh. 2024. Training-free Content Injection using h-space in Diffusion Models. In *Proceedings of the IEEE/CVF Winter Conference on Applications of Computer Vision*. 5151–5161.
- [26] Yifan Jiang, He Zhang, Jianming Zhang, Yilin Wang, Zhe Lin, Kalyan Sunkavalli, Simon Chen, Sohrab Amirghodsi, Sarah Kong, and Zhangyang Wang. 2021. Ssh: A self-supervised framework for image harmonization. In *Proceedings of the IEEE/CVF International Conference on Computer Vision*. 4832–4841.
- [27] Diederik Kingma, Tim Salimans, Ben Poole, and Jonathan Ho. 2021. Variational diffusion models. *Advances in neural information processing systems* 34 (2021), 21696–21707.
- [28] Gihyun Kwon and Jong Chul Ye. 2022. Clipstyler: Image style transfer with a single text condition. In *Proceedings of the IEEE/CVF Conference on Computer Vision and Pattern Recognition*. 18062–18071.
- [29] Mingi Kwon, Jaeseok Jeong, and Youngjung Uh. 2022. Diffusion Models Already Have A Semantic Latent Space. In *International Conference on Learning Representations*.
- [30] Jean-Francois Lalonde and Alexei A. Efros. 2007. Using Color Compatibility for Assessing Image Realism. In *IEEE International Conference on Computer Vision*. 1–8.
- [31] Yanghao Li, Naiyan Wang, Jiaying Liu, and Xiaodi Hou. 2017. Demystifying neural style transfer. In *Proceedings of the 26th International Joint Conference on Artificial Intelligence*. 2230–2236.
- [32] Jun Hao Liew, Hanshu Yan, Daquan Zhou, and Jiashi Feng. 2022. Magicmix: Semantic mixing with diffusion models. *arXiv preprint arXiv:2210.16056* (2022).
- [33] Chen-Hsuan Lin, Jun Gao, Luming Tang, Towaki Takikawa, Xiaohui Zeng, Xun Huang, Karsten Kreis, Sanja Fidler, Ming-Yu Liu, and Tsung-Yi Lin. 2023. Magic3d: High-resolution text-to-3d content creation. In *Proceedings of the IEEE/CVF Conference on Computer Vision and Pattern Recognition*. 300–309.
- [34] Chen-Hsuan Lin, Ersin Yumer, Oliver Wang, Eli Shechtman, and Simon Lucey. 2018. St-gan: Spatial transformer generative adversarial networks for image compositing. In *Proceedings of the IEEE/CVF Conference on Computer Vision and Pattern Recognition*. 9455–9464.
- [35] Tsung-Yi Lin, Michael Maire, Serge Belongie, James Hays, Pietro Perona, Deva Ramanan, Piotr Dollár, and C Lawrence Zitnick. 2014. Microsoft coco: Common objects in context. In *Computer Vision—ECCV 2014: 13th European Conference, Zurich, Switzerland, September 6–12, 2014, Proceedings, Part V 13*. Springer, 740–755.
- [36] Cheng Lu, Yuhao Zhou, Fan Bao, Jianfei Chen, Chongxuan Li, and Jun Zhu. 2022. Dpm-solver: A fast ode solver for diffusion probabilistic model sampling in around 10 steps. *Advances in Neural Information Processing Systems* 35 (2022), 5775–5787.
- [37] Lingxiao Lu, Jiangtong Li, Junyan Cao, Li Niu, and Liqing Zhang. 2023. Painterly image harmonization using diffusion model. In *Proceedings of the 31st ACM International Conference on Multimedia*. 233–241.
- [38] Shilin Lu, Yanzhu Liu, and Adams Wai-Kin Kong. 2023. Tf-icon: Diffusion-based training-free cross-domain image composition. In *Proceedings of the IEEE/CVF International Conference on Computer Vision*. 2294–2305.
- [39] Fujun Luan, Sylvain Paris, Eli Shechtman, and Kavita Bala. 2018. Deep painterly harmonization. In *Computer graphics forum*, Vol. 37. Wiley Online Library, 95–106.
- [40] Andreas Lugmayr, Martin Danelljan, Andres Romero, Fisher Yu, Radu Timofte, and Luc Van Gool. 2022. Repaint: Inpainting using denoising diffusion probabilistic models. In *Proceedings of the IEEE/CVF conference on computer vision and pattern recognition*. 11461–11471.
- [41] Chenlin Meng, Yutong He, Yang Song, Jiaming Song, Jiajun Wu, Jun-Yan Zhu, and Stefano Ermon. 2022. SDEdit: Guided Image Synthesis and Editing with Stochastic Differential Equations. In *International Conference on Learning Representations*.
- [42] Ben Mildenhall, Pratul P Srinivasan, Matthew Tancik, Jonathan T Barron, Ravi Ramamoorthi, and Ren Ng. 2021. Nerf: Representing scenes as neural radiance fields for view synthesis. *Commun. ACM* 65, 1 (2021), 99–106.
- [43] Alexander Quinn Nichol and Prafulla Dhariwal. 2021. Improved denoising diffusion probabilistic models. In *International conference on machine learning*. PMLR, 8162–8171.
- [44] Li Niu, Wenyan Cong, Liu Liu, Yan Hong, Bo Zhang, Jing Liang, and Liqing Zhang. 2021. Making images real again: A comprehensive survey on deep image composition. *arXiv preprint arXiv:2106.14490* (2021).
- [45] Hwai-Jin Peng, Chia-Ming Wang, and Yu-Chiang Frank Wang. 2019. Element-Embedded Style Transfer Networks for Style Harmonization. In *British Machine Vision Conference ,BMVC*.
- [46] Alec Radford, Jong Wook Kim, Chris Hallacy, Aditya Ramesh, Gabriel Goh, Sandhini Agarwal, Girish Sastry, Amanda Askell, Pamela Mishkin, Jack Clark, et al. 2021. Learning transferable visual models from natural language supervision. In

- International conference on machine learning*. PMLR, 8748–8763.
- [47] Robin Rombach, Andreas Blattmann, Dominik Lorenz, Patrick Esser, and Björn Ommer. 2022. High-resolution image synthesis with latent diffusion models. In *Proceedings of the IEEE/CVF conference on computer vision and pattern recognition*. 10684–10695.
 - [48] Nataniel Ruiz, Yuanzhen Li, Varun Jampani, Yael Pritch, Michael Rubinstein, and Kfir Aberman. 2023. Dreambooth: Fine tuning text-to-image diffusion models for subject-driven generation. In *Proceedings of the IEEE/CVF Conference on Computer Vision and Pattern Recognition*. 22500–22510.
 - [49] Yujun Shi, Chuhui Xue, Jiachun Pan, Wenqing Zhang, Vincent YF Tan, and Song Bai. 2023. DragDiffusion: Harnessing Diffusion Models for Interactive Point-based Image Editing. *arXiv preprint arXiv:2306.14435* (2023).
 - [50] Jiaming Song, Chenlin Meng, and Stefano Ermon. 2021. Denoising Diffusion Implicit Models. In *International Conference on Learning Representations*.
 - [51] Yang Song, Jascha Sohl-Dickstein, Diederik P Kingma, Abhishek Kumar, Stefano Ermon, and Ben Poole. 2021. Score-Based Generative Modeling through Stochastic Differential Equations. In *International Conference on Learning Representations*.
 - [52] Linfeng Tan, Jiangtong Li, Li Niu, and Liqing Zhang. 2023. Deep image harmonization in dual color spaces. In *Proceedings of the 31st ACM International Conference on Multimedia*. 2159–2167.
 - [53] Wei Ren Tan, Chee Seng Chan, Hernan Aguirre, and Kiyoshi Tanaka. 2019. Improved ArtGAN for Conditional Synthesis of Natural Image and Artwork. *IEEE Transactions on Image Processing* 28, 1 (2019), 394–409. <https://doi.org/10.1109/TIP.2018.2866698>
 - [54] Yi-Hsuan Tsai, Xiaohui Shen, Zhe Lin, Kalyan Sunkavalli, Xin Lu, and Ming-Hsuan Yang. 2017. Deep image harmonization. In *Proceedings of the IEEE Conference on Computer Vision and Pattern Recognition*. 3789–3797.
 - [55] Narek Tumanyan, Michal Geyer, Shai Bagon, and Tali Dekel. 2023. Plug-and-Play Diffusion Features for Text-Driven Image-to-Image Translation. In *Proceedings of the IEEE/CVF Conference on Computer Vision and Pattern Recognition (CVPR)*. 1921–1930.
 - [56] Ashish Vaswani, Noam Shazeer, Niki Parmar, Jakob Uszkoreit, Llion Jones, Aidan N Gomez, Lukasz Kaiser, and Illia Polosukhin. 2017. Attention is all you need. *Advances in neural information processing systems* 30 (2017).
 - [57] Huikai Wu, Shuai Zheng, Junge Zhang, and Kaiqi Huang. 2019. Gp-gan: Towards realistic high-resolution image blending. In *Proceedings of the 27th ACM international conference on multimedia*. 2487–2495.
 - [58] Yazhou Xing, Yu Li, Xintao Wang, Ye Zhu, and Qifeng Chen. 2022. Composite photograph harmonization with complete background cues. In *Proceedings of the 30th ACM international conference on multimedia*. 2296–2304.
 - [59] Xiao Yan, Yang Lu, Juncheng Shuai, and Sanyuan Zhang. 2022. Style Image Harmonization via Global-Local Style Mutual Guided. In *Proceedings of the Asian Conference on Computer Vision*. 2306–2321.
 - [60] Binxin Yang, Shuyang Gu, Bo Zhang, Ting Zhang, Xuejin Chen, Xiaoyan Sun, Dong Chen, and Fang Wen. 2023. Paint by example: Exemplar-based image editing with diffusion models. In *Proceedings of the IEEE/CVF Conference on Computer Vision and Pattern Recognition*. 18381–18391.
 - [61] He Zhang, Jianming Zhang, Federico Perazzi, Zhe Lin, and Vishal M Patel. 2021. Deep image compositing. In *Proceedings of the IEEE/CVF winter conference on applications of computer vision*. 365–374.
 - [62] Lingzhi Zhang, Tarmily Wen, and Jianbo Shi. 2020. Deep image blending. In *Proceedings of the IEEE/CVF winter conference on applications of computer vision*. 231–240.
 - [63] Richard Zhang, Phillip Isola, Alexei A Efros, Eli Shechtman, and Oliver Wang. 2018. The unreasonable effectiveness of deep features as a perceptual metric. In *Proceedings of the IEEE conference on computer vision and pattern recognition*. 586–595.
 - [64] Yuxin Zhang, Nisha Huang, Fan Tang, Haibin Huang, Chongyang Ma, Weiming Dong, and Changsheng Xu. 2023. Inversion-based style transfer with diffusion models. In *Proceedings of the IEEE/CVF conference on computer vision and pattern recognition*. 10146–10156.

A APPENDIX: ALGORITHM

The TF-GPH framework is based on stable-diffusion (SD) [47], combined with DPM-solver [36], which not only reduces the timestep requirements but also supports the functionality of the inversion process. And this inversion process can be further stabilized with a fixed prompt embedding ρ_{except} . We assume that the inversion process for the TF-GPH input has been completed. In the subsequent reconstruction stage, cross-image information is incorporated into the output image via our share-attention module. Our proposed share-attention module is a plug-and-play component, designed to replace the attention layer in the original SD framework. Furthermore, Our focus lies in the share-attention layer’s forward function (share-FORWARD), where we only substitute the forward mechanism of the original attention layer while retaining trained parameters (Q-K-V Projection layer, normalization layer, etc.). The detailed algorithm for TF-GPH is outlined in Alg. 1.

Algorithm 1: Training-and-prompt free General Painterly Harmonization

Data: initial noise $Z_T = \text{concat}\{z_T^{\text{ref}1}, z_T^{\text{ref}2}, z_T^{\text{comp}}\}$, step T_{share} and layer depth L_{share} to start using share attention module, the similarity weight $\hat{\alpha}$ and $\hat{\beta}$

Result: Harmonized Z_0

- ▶ We use default stable diffusion model with exceptional prompt embedding $\rho_{\text{exceptional}}$ as input, while rewriting the FORWARD of attention layer to Share-FORWARD
- ▶ We omit the linear transform and layer normalization, for brevity

```

1 Share-FORWARD( $Z_t, C, \hat{\alpha}, \hat{\beta}, t$ ):
2    $O_0 \leftarrow Z_t$ ;
3   for  $l = 0, 1, \dots, L$  do
4      $\hat{Q}, \hat{K}, \hat{V} \leftarrow \text{Proj}_l(O_l)$ ;
5     if  $t < T_{\text{share}}$  and  $l > L_{\text{share}}$  then
6       ▶ Start image-wise attention with reweighting
7       set  $(\alpha, \beta, \gamma)$  in  $\hat{M}$  to  $(\hat{\alpha}, \hat{\beta}, -\infty)$ 
8     else
9       ▶ Equivalent to normal diffusion process but in different shape
10      set  $(\alpha, \beta, \gamma)$  in  $\hat{M}$  to  $(-\infty, -\infty, 1)$ 
11    end
12     $\hat{A} = \text{Softmax}\left(\frac{\hat{M} \odot (\hat{Q}\hat{K}^T)}{\sqrt{d}}\right) \hat{V}$ ;
13     $O_l \leftarrow O_l + \hat{A}$ ;
14    ▶  $CA_l$  is the cross-attention layer at layer  $l$ ,  $C$  is the corresponding text embedding (fixed to  $\rho_{\text{exceptional}}$ )
15     $O_{l+1} \leftarrow O_l + CA_l(O_l, C)$ ;
16  end
17  return  $O_L$ ;

```

B APPENDIX: DATASETS

B.1 WikiArt [53] with COCO [35].

This dataset has been widely adopted by various general stylization methods [5, 12, 23, 37] due to its high flexibility and feasibility. Following common evaluation practices, we utilize the WikiArt dataset for background images and the COCO dataset as the source for foreground objects. Specifically, we randomly sampled 1000 images from the WikiArt validation dataset and 1000 segmented objects across 80 different classes from the COCO validation dataset (with each object’s class equally distributed). These segmented objects are then composited onto the background images to generate our final composite images. (The evaluation result can be found in Fig. 16, Tab. 4). However, a limitation of this dataset lies in its diversity, which is constrained to combinations of real-world objects (from COCO) against paintings (typically European style). As a result, the data distribution from WikiArt combined with COCO may not fully represent real-world applications of image harmonization tasks, which often involve combining fictional objects with various forms of graphic art.

B.2 TF-ICON Benchmark [38].

This dataset was originally designed for prompt-based image composition, with each data entry containing four components: a text-generated background image, a reference image of a real-world object, a composite image of the real-world object with the background, and a prompt describing the composite image. The background images encompass four visual domains: cartoon, photorealism, pencil sketching, and oil painting. For evaluate the prompt-free ability of our proposed TF-GPH method, **we omit the given text descriptions and only use the images as input**. The evaluation result can be found in Fig. 8 and Tab. 2. While this benchmark provides an additional prompt for more flexible evaluation, it lacks diversity as the backgrounds are all images produced by a generative model for the purpose of aligning prompt description to background style, lacking data of real-world paintings such as famous paintings "Starry Night," which are widely adopted in real-world stylized applications.

B.3 General Painterly Harmonization Benchmark.

We have observed the drawbacks of the aforementioned dataset-lacking strong correlation toward the usage of image composition related tasks in real-world applications. Hence, we propose the General Painterly Harmonization Benchmark (GPH-Benchmark), aiming to solve not only the generalizability issues of existing datasets but also the shortcomings of current evaluation metrics by computing the content/stylized range as an approximation of harmonization ability. Beginning with the construction of the dataset, our objective is to generalize three main applications commonly used by human users in real-world scenarios: **object swapping**, **object insertion**, and **style transfer**. Our dataset comprises source data from real-world objects, generated objects, famous painterly backgrounds, and generated backgrounds with unique styles, resulting in a total of 635 test cases that cover various examples of

general painterly harmonization created by human labor. We partition the conventional painterly image harmonization task into two distinct subcategories: object swapping and object insertion. The primary distinction lies in the objectives pursued by each subcategory. Object swapping aims for high-level semantic harmonization, emphasizing strong semantic connections between the swapped object and the background image. For instance, in the case of swapping faces, the goal is to ensure natural integration with surrounding features like hair and skin color. On the other hand, object insertion prioritizes low-level visual naturalness, focusing on harmonizing edges and textures to achieve visual coherence.



Figure 7: The demo of GPH-Benchmark, consisting of more general test data falling out of distribution of previous training-required methods [37, 38, 41]. First row: "insert object", "background", "Ours". Second row: "TF-ICON" [38], "PHDiff" [37], "SDEdit" [41]

C APPENDIX: BASELINES

PHDiffusion [37]: PHDiffusion (abbreviated as PHDiff in subsequent sections) is a framework for painterly harmonization. They propose incorporating an additional adaptive encoder combined with a fusion module into the existing stable diffusion pipeline and fine-tuning this combined pipeline on the WikiArt with COCO dataset. It is noteworthy that within this framework, they introduce an additional "Strength" hyperparameter to control the scale of the fusion module, which also represents the influence of the background style on the pasted object. Consequently, to evaluate the performance of the content emphasis strategy of PHDiff, we set the 'Strength' parameter to 0, while for the stylization emphasis strategy, we set it to 1. (Their default setting for 'Strength' is fixed at 0.7).

TF-ICON [38]: The TF-ICON approach primarily leverages two hyperparameters to govern the prompt-based image composition process. Firstly, τ_α indicates the onset of attention injection (0 for beginning, 1 for the end), and secondly, τ_β denotes the onset of the rectification process. Unfortunately, neither τ_α nor τ_β directly modulates stylization intensity. However, reducing τ_α generally yields more stylized outputs, while reducing τ_β produces images closer to the composite. Thus, to assess TF-ICON's content emphasis

strategy, we follow the setting suggest by TF-ICON, we set $\tau_\alpha = 0.4$ and $\tau_\beta = 0$ as proposed in their paper for photography composition, demanding heightened content preservation. Conversely, for the stylization emphasis strategy, we adopt $\tau_\alpha = 0.4$ and $\tau_\beta = 0.8$ as recommended for cross-domain composition, necessitating higher stylization strength.

VCT [9]: The VCT method utilizes a set of specially designed loss to fine-tune the given stable-diffusion model with one-shot style reference. Consequently, the longer the tuning process takes, the more the SD model fits to the given style. Thus, to assess VCT's content emphasis strategy, we directly discard the tuning process using default SD model for reconstruction, as for the stylization emphasis strategy, we simply leverage their default hyperparameters for tuning, which take around 5 to 10 minutes tuning process for a single RTX 3090 GPU on each test sample (while the inference time for single image usually take 5 to 30 seconds).

D APPENDIX: MORE QUALITATIVE RESULT

D.1 Qualitative of WikiArt w/ COCO

We provide the comparison of our proposed method toward other baselines in Fig. 16.

D.2 Qualitative of TF-Benchmark

We provide the comparison of our proposed method toward other baselines in Fig. 8.



Figure 8: Results on TF-Benchmark. Our results (second row) show better content preservation than TF-ICON (first row).

D.3 More Qualitative result of GPH Benchmark

We provide more result of TF-GPH on GPH Benchmark in Fig. 17 (Insertion and swapping) and Fig. 18 (Style Transfer).

E APPENDIX: MORE QUANTITATIVE RESULT

E.1 Quantitative of WikiArt w/ COCO

We provide the comparison of range-based evaluation on WikiArt combined with COCO in Tab. 4.

F APPENDIX: USER STUDY

Survey flow. At the outset, each participant will receive instructions and a demonstration question aimed at familiarizing them

with the answer flow and evaluation criteria ("Content Consistency," "Style Similarity," "Visual Quality"). Subsequently, they will be required to answer 10 randomly selected questions from a pool of 30 questions, along with an attention-check question designed to assess the validity of their responses (details provided in the following section). Furthermore, the options for each question will be shuffled for enhanced reliability. The participant’s view of the question is illustrated in Fig. 9.

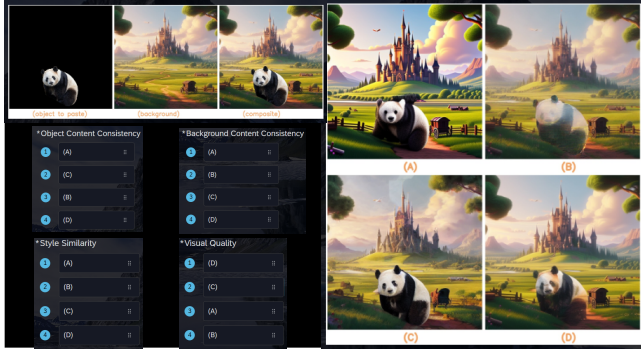


Figure 9: A painterly harmonization question participant might need to answer.

Attention-check question. The intent behind these questions is to confirm the participant’s grasp of the concepts of "content consistency" and "style similarity." For instance, within the construction of attention-check questions for the style transfer task, we provide the content reference and style reference directly, expecting them to be ranked at first place for "content consistency" and "style transfer," respectively, by the participant. As illustrated in Fig. 10, where the participant should rank (C) in the first place of content consistency, and (D) in the first place of style similarity. We reject the responses that fails the attention check and collect 50 valid responses for each painterly harmonization and style transfer task.

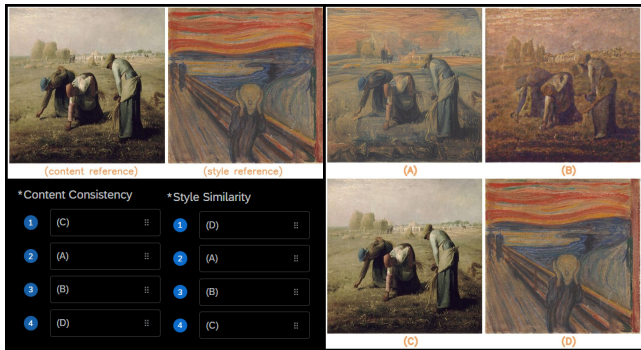


Figure 10: The attention-check question for style transfer task.

G APPENDIX: MORE EXPERIMENT

G.1 Experiment of Inference-time-adjustable Hyperparameters

The TF-GPH incorporates four adjustable hyperparameters during inference: T_{share} , T_L , α , and β . The initial two parameters, T_{share} and T_L , govern the commencement timing of the share-attention layer; an earlier start of the share-attention layer leads to increased blending of objects into the background. Meanwhile, the latter two parameters, α and β , regulate the weighting of references in the reconstruction process; decreasing α and increasing β result in a more stylized output. These adjustments afford TF-GPH enhanced adaptability across a diverse array of usage scenarios. We present a straightforward visualization depicting the shift in quantitative indices solely by varying T_{share} in Fig. 11, alongside the qualitative outcome of altering others Fig. 12 and Fig. 13.

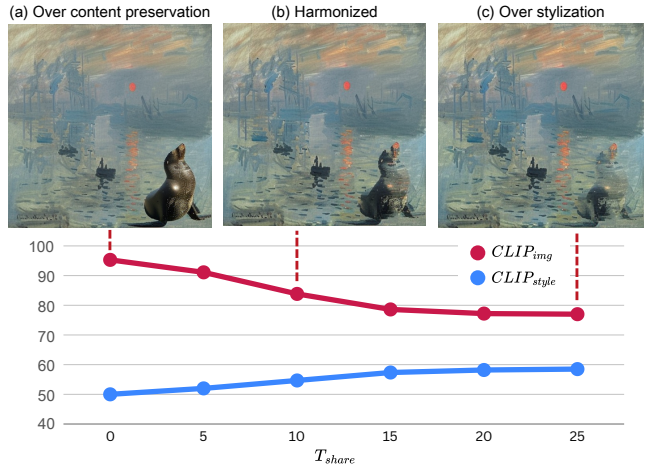


Figure 11: Comparison of different stylized strength, when adjusting T_{share} only.

H APPENDIX: MORE APPLICATIONS

H.1 Inpainting

We incorporate our proposed share-attention w/ reweighting into the inpainting method Repaint[40]. And provide the functionality of exemplar guided inpainting. We replaced the noisy latent inside mask area of z_T^{comp} to the noise of z_T^b . The result can be found in Fig. 14, showing that our proposed method is able to provide current inpaint method additional exemplar information based on existing framework.

H.2 Semantic mixing

We test the compatibility of share-attention layer with semantic mixing method InjectFusion [25], which is the adaption of the renowned Asyrp[29] approach. The core concept shared by these methods involves blending the semantic information from two images by manipulating their h-space, specifically the intermediary attention layer within the diffusion UNet architecture. To integrate the shared-attention layer into the InjectFusion, we simply allow

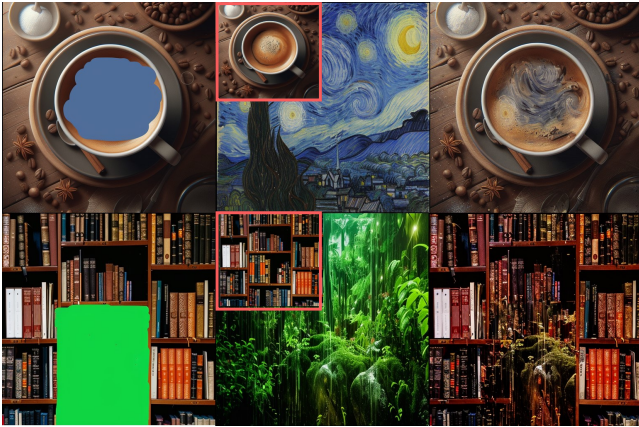


Figure 14: The left column is the given I^{comp} and corresponding inpaint mask, the middle column is the additionally provided I^f (in red box) and I^b . The last column is the output image.



Figure 15: The columns, from left to right, represent I^f , I^b , and I^o , where our share-attention layer is able to perform astonishing semantic mixing when combined with corresponding method.

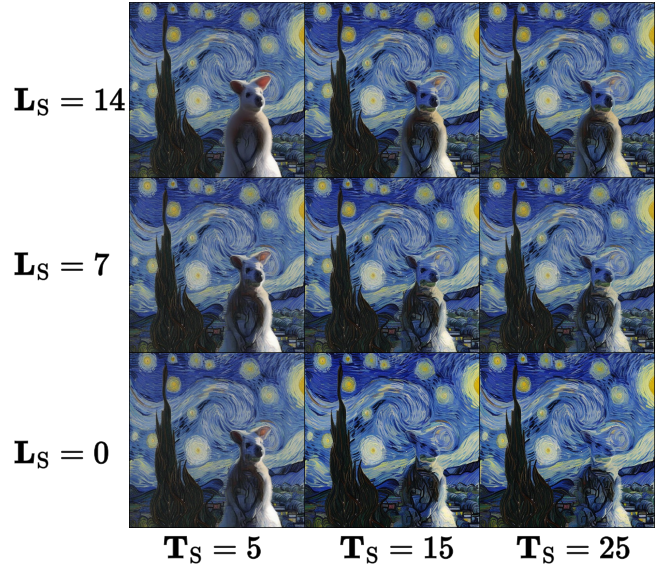


Figure 12: Comparing various levels of stylized strength by adjusting both T_{share} and L_{share} (abbreviated as "S"), with fixed values for $\alpha = 0.9$ and $\beta = 1.1$.

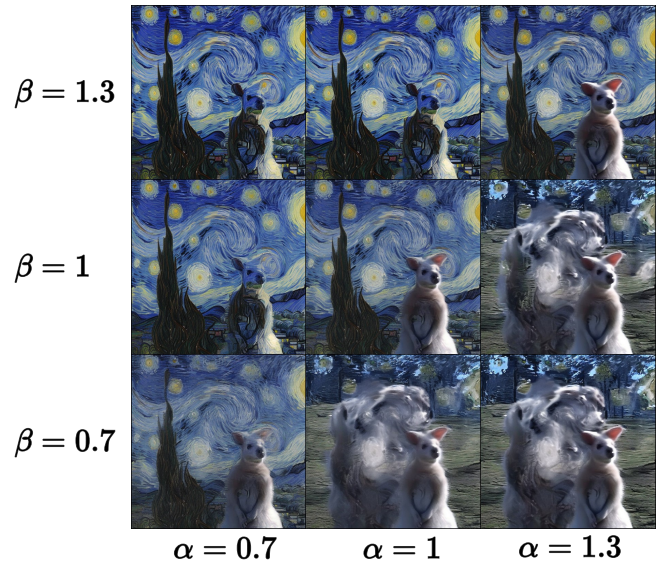


Figure 13: Comparing various levels of stylized strength by adjusting both α and β , with fixed values for $T_{\text{share}} = 15$ and $L_{\text{share}} = 7$.

the output image to attend to additionally provided I^b via our share-attention layer. The generated result can be found in Fig. 15

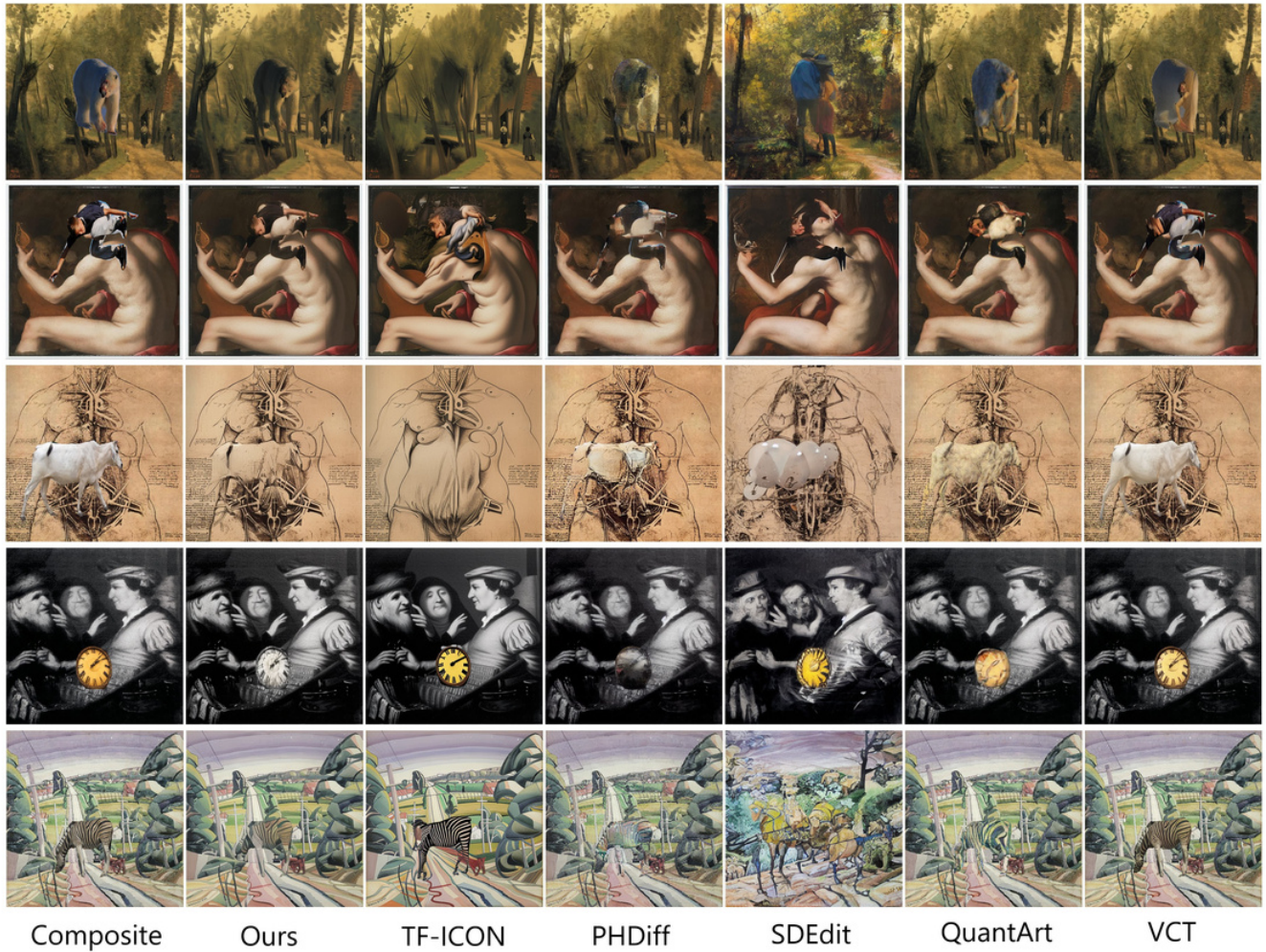


Figure 16: Qualitative comparison of WikiArt combined with COCO

Table 4: Quantitative comparison of WikiArt combined with COCO

	Composite	Ours (low/high)	Painterly Harmonization					Style Transfer Harmonization		
			TF-ICON	PHDiff	PHDNet	SDEdit	DIB	QuantArt	VCT	StyTr ²
<i>Venue</i>	-	-	ICCV'23	MM'23	AAAI'23	ICLR'22	WACV'20	CVPR'23	ICCV'23	CVPR'22
$LPIPS_{bg} \downarrow$	0	0.08/0.10	0.21/0.34	0.08/0.11	0.34	0.36	0.11	0	0	0
$LPIPS_{fg} \downarrow$	0	0.10/0.27	0.30/0.35	0.11/0.30	0.32	0.29	0.23	0.28	0.12	0.16
$CLIP_{img} \uparrow$	99.99	92.88/80.40	83.79/82.65	91.78/80.32	81.65	80.70	88.43	81.22	90.86	87.43
$CLIP_{style} \uparrow$	45.60	47.96/ 55.25	49.51/50.02	46.17/53.95	50.64	50.46	48.59	50.02	47.85	50.31
$CLIP_{dir} \uparrow$	0	5.44/ 19.20	7.63/11.18	6.49/18.14	15.80	13.46	8.67	15.23	6.26	11.16

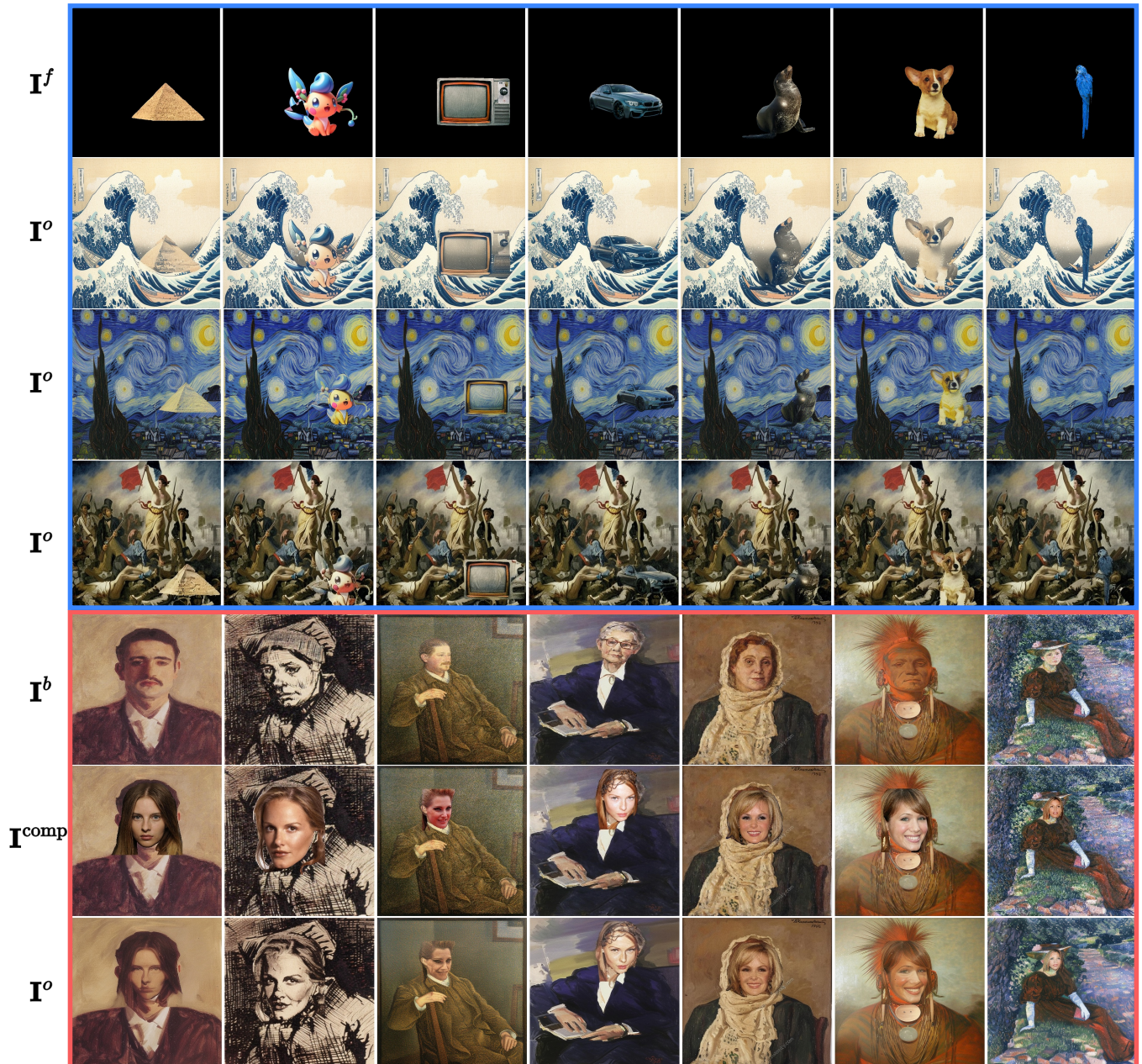


Figure 17: More painterly harmonization result of our proposed TF-GPH on GPH Benchmark. The row 1, is the input foreground objects, and the row 2,3,4 are the corresponding outputs, The row 5 is the input background objects, the row 6 is the composite image with given face to paste, and the row 7 is the corresponding outputs

Changing Style

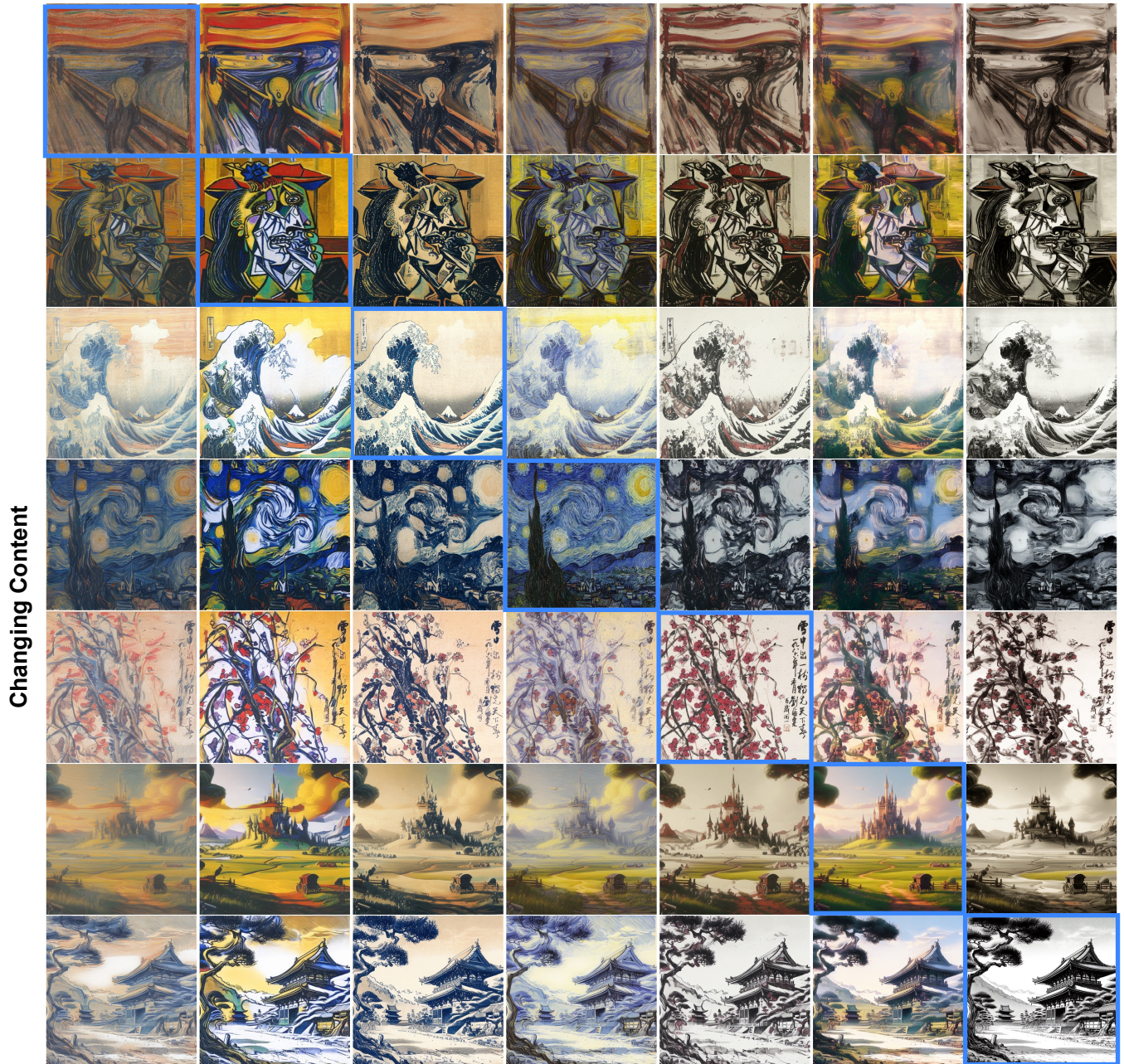


Figure 18: More style transfer result of our proposed TF-GPH on GPH Benchmark. The images inside blue box, serves as both the content reference for the corresponding row and the style reference for the corresponding column,